Comments on the analysis of tritium content in electrochemical cells

S. Szpak, P.A. Mosier-Boss and R.D. Boss
Naval Command, Control and Ocean Surveillence Center RDT&E Division, San Diego, CA 92152-5000 (USA)

J.J. Smith
Department of Energy, Washington, DC 20585 (USA)

(Received 12 July 1993; in revised form 10 November 1993)

1. INTRODUCTION

Following the report by Fleischmann and Pons [1] in 1989 that nuclear events, including the production of tritium, can be initiated in electrochemical cells during the electrolysis of heavy water on Pd cathodes, tritium production has been claimed in a number of publications, a list of which was compiled by Storms [2] and more recently reviewed by Chien et al. [3]. However, substantial difficulties have been encountered in reproducing reported data and considerable controversy remains concerning the occurrence of such events, including tritium production.

Tritium production is typically ascertained from its distribution among the cell components during prolonged electrolysis. The tritium production rate, if any, can best be examined in closed cells and determined from a total mass balance [4]. However, the majority of researchers use open cells where the rate of tritium production is calculated from enrichment in the electrolyte phase, the gaseous phase or both. This enrichment is often computed under conditions of constant electrolyte volume which implies continuous additions and withdrawals of electrolyte, a somewhat unrealistic undertaking. Most reported instances of tritium production involve low levels (e.g. of the order of 10^4–10^5 atoms S^{-1} cm^{-2} [4]; data analysis at such levels requires extreme care, particularly in open–cell experiments.

In this paper we examine the limitation(s) of commonly used expressions for the distribution of tritium in the gas and liquid phases during prolonged electrolysis and comment on the methodology of data acquisition. Furthermore, we emphasize the difficulties that may arise in interpreting the results obtained by these procedures. We note that these expressions were derived for the simplest model of deuterium evolution on D–saturated Pd electrodes.

2. DERIVATION OF EXPRESSIONS—MASS BALANCE CONSIDERATION

The fluxes associated with the electrolysis of water in cells employing hydrogen–absorbing cathodes [5], are summarized in Fig. 1. The gaseous products generated during electrolysis of heavy water, i.e. D_2 and/or DT evolving at the cathode C and O_2 at the anode A, are catalytically recombined in a separate vessel R. Because of the absorption of hydrogen isotopes by the cathode material, the hydrogen flux produced by electrolysis is divided into three streams: entering the electrolyte by the Heyrovsky–Horiuti path oi' other exchange processes, entering the gaseous phase (recombiner) by the Tafel path and entering the bulk electrode by absorption. If tritium is produced (consumed) during the experiment, either the magnitude of these fluxes changes or other appropriate fluxes should be considered. The mass balance can be written for the closed system (total mass balance) or, for greater flexibility in the experimental arrangement and data interpretation, separately for each part of the system (the electrolyte, the recombiner and the electrode). The mass balance of tritium in the electrolyte is of special interest since conclusions have often been based on measurements of the electrolyte phase [2.3].

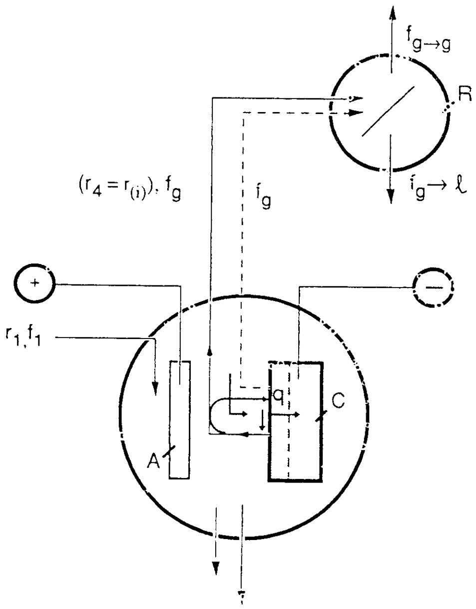

Figure 1. Mass balance on electrolyte: *r*, rates of mass change (subscripts 1, 2, 3 and 4 indicate electrolyte addition, removal by sampling, evaporation and electrolysis respectively); *f*, tritium mass fraction (subscripts g and l denote gas and liquid phases); cell components are shown by bold lines (A, anode; C, cathode; R, recombiner); concentration is schematic.

The time dependence of tritium concentration in the electrolyte phase is calculated by solving the equation

$$\frac{d(fm)}{dt} = \sum_n f_n r_n + kq \quad n = 1, 2, ... \tag{1}$$

subject to experimental conditions specified by

$$\frac{dm}{dt} = \sum_n r_n \tag{2}$$

where f denotes the tritium mass fraction, m is the mass of electrolyte and the subscript n identifies the relevant process. Specifically, r_1 is the rate of D_2O addition to replenish that removed by electrolysis, r_2, r3 and r_4 (also called *r(i))* are the rates of removal due to sampling, evaporation and electrolysis respectively, and kq ($k \leq 1$) is that fraction of tritium, produced or consumed in the electrode interior q, that has been transferred to the electrolyte phase irrespective of the transport mode. As written, eqn. (1) implies that if tritium is generated within the electrode, it is transferred to the electrolyte phase or if it is consumed, it is removed from the electrolyte phase. Tritium balance on the recombiner and electrode are formulated in an analogous manner with the inclusion of the relevant fluxes identified in Fig. 1.

Substitution of *(2)* into (1) yields an equation of the type

$$\frac{dy}{dt} + P(t)y = Q(t)$$

which has the solution

$$y = y(0)\exp\left[-\int_0^t P\,dt\right] + \exp\left[-\int_0^t P\,dt\right]\int_0^t Q\exp\left[\int_0^t P\,dt\right]dt \tag{3}$$

2.1. Tritium in the Electrolyte Phase

Analytical solutions of eqn. (3) describing tritium concentration in the electrolyte phase for two experimental procedures, i.e. constant electrolyte volume and intermittent sampling, are as follows.

2. 1.1. Open Cell and Constant Electrolyte Volume. When the cell is operated at constant mass of electrolyte, i.e. compensating for all losses by a continuous supply of electrolyte, we have (note that since $dm/dt = 0$, $m(t)=m(0)$)

$$m(0)\frac{df}{dt} + sf[r(i) + r_2] = f_1 r_1 + kq \tag{4}$$

where we have taken $sf = f_2$, where s is the isotopic separation factor (see Section 4.2 for further discussion). With $P = s[r(i) + r_2]/m(0)$ and $Q = (f_1 r_1 + kq)/m(0)$, the solution of eqn. (4) is

$$f = f(0)\exp^{(-t/\tau)} + \frac{f_1 r_1 + kq}{sr(i) + r_2}[1 - \exp^{(-t/\tau)}] \tag{5}$$

where $\tau = m(0)/(sr(i) + r_2)$. When additional constraints are imposed, e.g., $r_1 = r(i)$, $r_3 = 0$, $f_1 = f(0)$, we obtain

$$f = f(0)\exp^{(-t/\tau)} + \frac{f(0)}{s}[1 - \exp^{(-t/\tau)} + \frac{kq}{sr(i)}[1 - \exp^{(-t/\tau)}] \tag{6}$$

Rearranging eqn. (6), we obtain

$$\frac{f}{f(0)} = s - (s - 1)\exp^{(-t/\tau)} + \frac{kq}{sr(i)f(0)}[1 - \exp^{(-t/\tau)}] \quad \tau = \frac{m(0)}{sr(i)} \tag{7}$$

which is the form employed by Lin et al. (6) and Adzic et al. (7), with the last term determining the generation rate. In this formulation, the difference between the calculated distribution, without the production term, and the experimentally observed concentration is attributed to tritium generation, in particular to that portion that has been transferred to the electrolyte phase. The isotopic separation factor s employed here is defined in terms of the D/T atomic ratio.

A plot of tritium concentration in the electrolyte phase versus dimensionless time t/τ is shown in Fig. 2, curve (a), for q = 0, while that in the “electrolytic” gas phase is shown by curve (a′). Suppose that at $t/\tau = 1$ (point A) a continuous production of tritium is initiated; the net result is new curves (b) and (b′) for the electrolyte and recombined phases respectively. These curves are analogous to curve (a) but asymptotically approach the value $s + kq/sr(i)f(0)$. If, as reported [2,3], tritium production is a burst–like event followed by direct transfer to the gas phase, then the situation is different, i.e. the build–up in the electrolyte phase remains unchanged (curve (c)) but the tritium concentration in the gas phase is displaced (curve (c′)) which would effectively change the value of the separation factor s. While these results are interesting, the model assumes experimental conditions of known concentration of tritium in the electrolyte, without requiring sampling, and constant volume (i.e. $r_2 = 0$ and $r_1 = r(i)$). Neither of these assumptions is physically reasonable and, in practice, they are not usually met. These considerations lead to the following much more realistic case of intermittent sampling and addition.

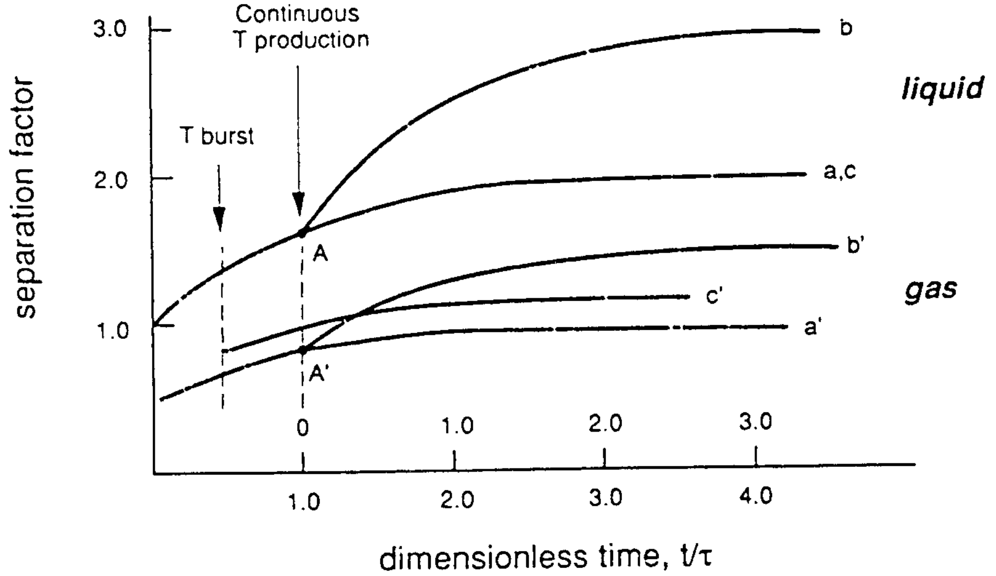

Figure 2. Calculated tritium distribution between the electrolyte and “electrolytic” gas phase as a function of dimensionless time (calculations for s = 2): (a), (a′) liquid and gas phases for $q = 0$; (b), (b′) liquid and gas phases for $q > 0$; (c′) gas phase enrichment by pulse production, as indicated.

2.1.2. Open Cell and Intermittent Sampling. A more realistic sampling procedure is illustrated in Fig. 3, from which the tritium concentration in open cells is calculated as follows. An initial charge $m(0)$ is electrolyzed at a constant cell current I for a specified time t, when a sample is withdrawn (to be analyzed for tritium), after which D_2O is added to restore the original volume. Thus the rates r_1 and r_2 are zero, except when solvent is added or sample is removed, and $r(i)$ is constant for a constant cell current (Faraday law). If the radioactive decay (ca. 0.5% per month) and the loss by evaporation are neglected, the time rate of change of tritium content between sampling is obtained by substituting eqn. (2), with $r_1 = 0$ and $r_2 = 0$, into eqn. (1) and solving the resulting eqn. (3) which, with $P = (s - 1)r(i)/[m(0) — r(i)t]$ and $Q = kq(t)/[m(0) — r(i)t]$, yields

$$f(t) = [m(0) - r(i)t]^{s-1} \times \left[\frac{f(0)}{m(0)^{s-1}} + \int_0^t \frac{kq(t)}{[m(0) - r(i)t]^s} dt \right] \tag{8}$$

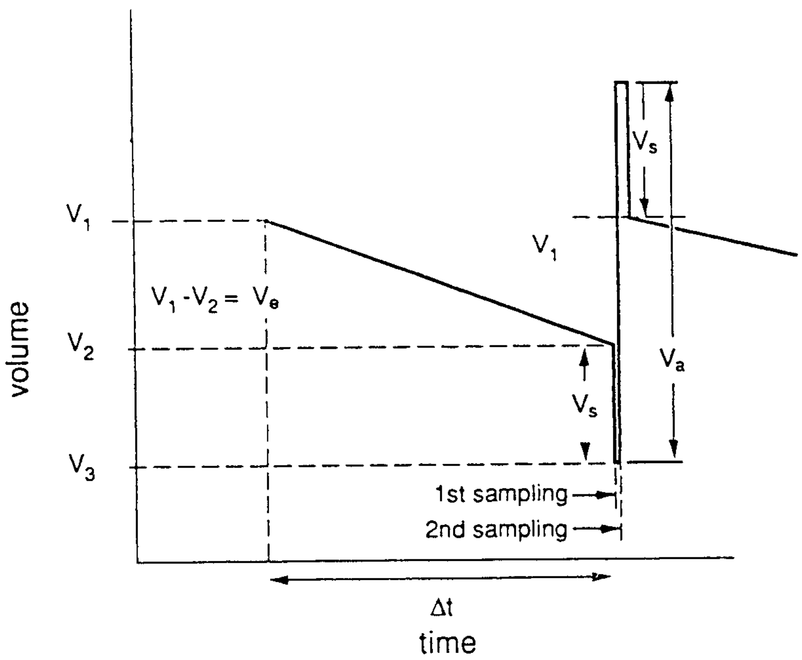

Figure 3. Sampling procedure for tritium generation in open cells: $V_{e[} = IM_{D_2O}\Delta t/2F_p$ is the volume lost by electrolysis; V_S is the sampling volume; V_a is the electrolyte volume added to restore prior conditions.

In practice, when using eqn. (8) and assuming that the generation rate q is constant, the integral $\int_0^t [m(0) - r(i)t]^s dt$ can be treated as a weighting factor. For kq = const, eqn. (8) can be written as

$$f = f(0)\left[\frac{m(0) - r(i)t}{m(0)}\right]^{s-1} + \frac{kq}{(s-1)r(i)}\left\{1 - \left[\frac{m(0) - r(i)t}{m(0)}\right]^{s-1}\right\} \tag{9}$$

Equations (7) and (9) both suggest that the evidence for tritium production can be obtained by determining its concentration in the electrolyte phase alone, but only if the isotopic separation factor s is either constant or a known function of time. Plots of tritium distribution and build–up as a function of time as predicted by eqns. (7) and (9) are shown in Fig. 4. Curve (a′) illustrates the time dependence of eqn. (7) corrected for sampling. Curve (b) is the time dependence predicted by eqn. (9). As can be seen, curves (a’) and (b), when properly corrected for sampling effects, are nearly equivalent; hence either equation can be used for data analysis.

2.2. Balance on Recombiner

Because of the conditions imposed, i.e. constancy of the separation factor and a relatively low rate of tritium production [4], the mass balance on the recombiner can provide additional information. The tritium mass balance on the catalytic converter, working with an efficiency ε_r, is given in terms of the tritium mass fraction:

$$f_g = \epsilon f_{g\to 1} + (1 - \epsilon_r) f_{g\to g} \tag{10}$$

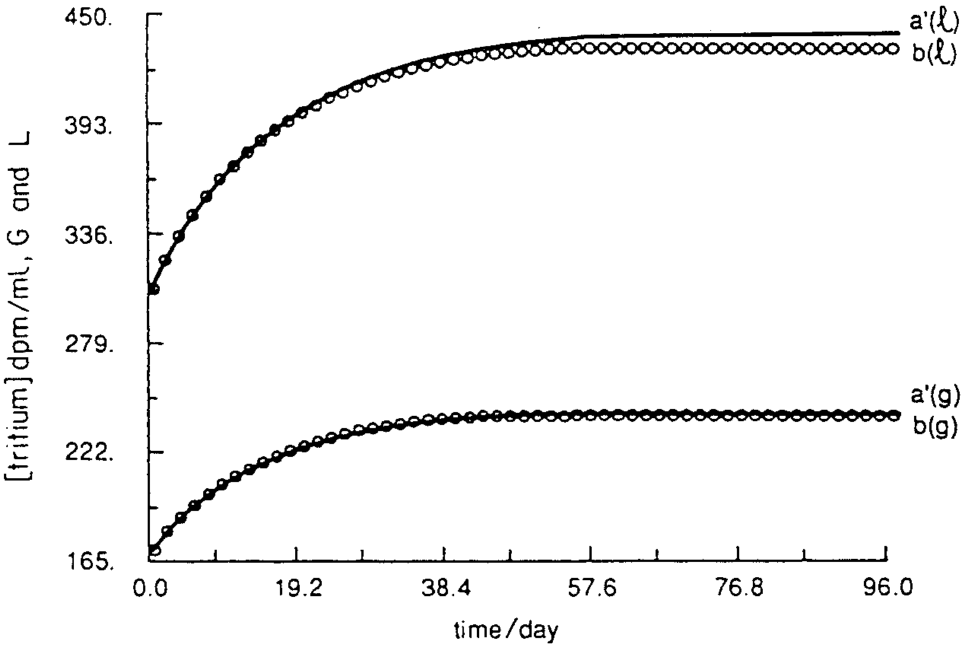

Figure 4. Calculated tritium distribution (simulated data) between “electrolytic” gas and electrolyte phases as a function of time: (a′) time dependence of eqn. (7) corrected for dampling; (b) time dependence of eqn. (9). Input data: $s = 1.8$; initial $[^3H] = 300$ dpm ml^{-1}.

where subscript g → l refers to the mass fraction found in the liquid collected during catalytic conversion and g → g indicates the fraction that is lost due to the inefficiency of the recombiner. Assuming perfect mixing in the catalytic converter and recognizing that the rate of reaction of D_2 with O_2 is faster than that of DT, we must introduce a second separation factor, i.e. $s* = f_{g\to 1}/f_{g\to g}$, which, when substituted into eqn. (11), yields

$$f_g = f_{g\to 1}\left(\epsilon_r + \frac{1-\epsilon_r}{s*}\right) \tag{11}$$

Since $s*$ is not generally known, care must be taken to provide a sufficiently large catalyst area to match the rate of recombination with the rate of the gas evolution, so that $\epsilon_{r\to 1}$, thereby removing the term which contains $s*$. Failure to do so would produce a systematic underestimation of the tritium content in the gas phase.

3. DATA ACQUISITION–EXPERIMENTAL PROCEDURE

In principle, any cell design may be employed. In practice, cells are usually constructed in such a manner as to provide a uniform current density distribution on the Pd cathode which is totally immersed in an electrolyte. Operating cells are considered to be open systems if the evolving gases are allowed to escape and/or are catalytically recombined in a separate compartment. The solvent evaporation rate must be minimized by either installing a reflux condenser or providing a cooling jacket. In what follows, uncertainties associated with tritium analysis and sampling procedure are assessed.

3.1. Tritium Analysis

The commonly used analytical procedure employed to measure tritium content is the liquid scintillation technique. In this technique, a sample is added to a scintillation cocktail (e.g. Fisher

Scientific ScintiVerse E Universal LSC Cocktail). The prepared solutions are then counted for a given amount of time, depending upon the accuracy required, in a scintillation counter such as the Beckman LS 6000 LL. Care must be taken to ensure stabilization and adequate compensation for chemiluminescence and photoluminescence. Samples containing dissolved Pd^{2+} ions should first be distilled to dryness before the distillate is added to the scintillation cocktail. Chemiluminescence from alkaline solutions can be eliminated by the addition of glacial acetic acid. Shielding in the detector compartment is necessary to reduce the cosmic–ray–induced γ–ray background.

We have determined the accuracy of this method using replicate samples; the results are summarized in Table 1. As can be seen, the results all fall within ± 1 standard deviation. It should be noted that count times depend on the concentration of tritium. For example, high levels of T, such as are present in samples from Cambridge Isotopes Laboratories Ltd. (ca. 350 dpm ml^{-1}) require times of about 200 min, while D_2O samples with low tritium concentrations (e.g. those from Isotec Inc.) require longer count times for the same accuracy.

Table 1. Error estimate for tritium content in heavy water.

Sample	$[^3H]/dpm\ ml^{-1}$	
	A	*B*
1	346	19.6
2	343	18.9
3	343	19.7
4	345	19.0
5	346	18.5
Average	345 ± 4	19.1 ± 1.2

A, D_2O with high ^3H content (source: Cambridge Isotopes, lot no. F 3791), counting time 240 min.
B, D_2O with low ^3H content (source: Isotec Inc., lot no. PV 0651), counting time 600 min.
Error in counting efficiency: A, ± 4; B, ± 1.2.

3.2. Sampling Procedure

A sampling procedure is illustrated in Fig. 3. Initially, an electrolyte of known tritium content is placed in an electrochemical cell and electrolyzed at constant cell current I for a time period t. At this time, a known volume of electrolyte is removed and analyzed for tritium content. The electrolyte volume is adjusted and a second sample is removed for tritium analysis. In this manner, the electrolyte volume and concentration are accurately known for the beginning of the next time interval. Concurrently D_2, DT and O2 gases are catalytically recombined to form D_2O (or DTO) and the resulting liquid is collected in a separate vessel for tritium analysis. The design of the recombining vessel must assure that the samples taken out for tritium analysis are representative of the total D_2O and DTO recombined throughout a given time interval.

In addition to analytical errors (Table 1), there are uncertainties in the electrolyte volume owing to sampling as well as the constancy of cell current and measurements of the time intervals. To illustrate the magnitude of these uncertainties, a representative sample of data from several experiments is assembled in Table 2 for the sampling procedure described in Fig. 3. The first column lists the electrolyte volume V_1 at the beginning of a particular time period. This initial volume is reduced to V_2 by electrolysis at the cell current I for a time interval Δt, and by sampling to V_3. To restore the electrolyte volume, an additional volume V_a of D_2O with a known tritium content is added and, after mixing, a second sample is removed from the cell for analysis. The remaining volume is the new initial volume V_1 for the next time interval. It should be noted that the second sample provides a means by which to estimate the magnitude of the sampling errors, as shown by the calculated and observed tritium content (Table 2, columns 5 and 6). The data in Table 2 indicate that the greatest source of error in these analyses is due to the uncertainty in the tritium measurement itself and not the volume measurements.

Table 2. Error estimate in initial conditions (volume) by tritium content measurements.

V_1/ml	$10^{-5}\ I\Delta t$/As	V_2/ml	V_a/ml	$[^3H]$/dpm ml^{-1}	
				Observed	Calculated
40.30 ± 0.06	7.41	36.15 ± 0.08	8.89 ± 0.01	16.1 ± 1.2	15.8 ± 1.0
39.47 ± 0.08	6.284	35.94 ± 0.09	11.85 ± 0.01	15.2 ± 0.9	15.9 ± 1.1
41.84 ± 0.17	6.045	38.45 ± 0.17	5.93 ± 0.01	18.9 ± 1.2	18.5 ± 0.9
50.31 ± 0.05	10.28	44.54 ± 0.05	8.21 ± 0.01	411 ± 4	412 ± 4
47.89 ± 0.06	11.72	41.31 ± 0.06	6.59 ± 0.01	425 ± 4	424 ± 4

Uncertainties: time, ±10 s, cell current I, ±0.001 A. Syringes for sample removal and D_2O addition were calibrated prior to use to minimize volume errors; the largest source of error is the tritium measurement itself.

These experiments typically run for a month or more. The first three rows are results from an experiment using low tritiated D_2O. We are showing the results from three different days, or time intervals, during the course of that experiment. The last two rows are from an experiment using D_2O with a higher initial tritium content and the results tabulated are from two different time intervals.

The uncertainties in V_1 and V_2, the volumes at the beginning and end of a time interval Δt, reflect the propagation of error from prior samplings.

4. RESULTS AND DISCUSSION

Two approaches to the interpretation of the data are considered: a curve–fitting technique and a comparison of calculated and observed values. As written, eqn. (2) specifies the sampling procedure, thereby indicating whether eqn. (7) or eqn. (9) is more suitable. For example, the necessary condition leading to eqn. (7) is the maintenance of a constant electrolyte volume throughout the duration of an experiment. In practice, this condition is violated by sampling and electrolysis. However, there is no need to maintain the electrolyte volume constant when employing eqn. (9). The only requirement is that the values for the volume, tritium content and cell current be known accurately at the beginning of each time period.

4.1. Curve–Fitting Technique

In general, curve–fitting techniques are adequate when simple and clearly defined models describe the physical situation and when large amounts of data have been collected, typically over a long period of time. Below, we apply curve fitting to determine whether it is useful in the analysis of the tritium concentration data.

Equation (9) has two adjustable parameters which are coupled to one another, namely, the isotopic separation factor s and the tritium generation rate q. We have tested the evaluation of these quantities by applying a computer—aided analysis utilizing, for example, the Nelder–Mead algorithm which adjusts these parameters in such a way as to minimize the sum of the squares of the residuals. In a general case, two additional parameters associated with experimental procedures should be included, namely the faradaic and recombining efficiencies ε_f and ε_r. The first parameter arises from the reduction of oxygen generated at the anode and dissolved in electrolyte; the second is due to differences in the kinetics of the reaction of D_2 and DT molecules with oxygen.

To assess the usefulness of the curve–fitting technique, simulated data for tritium in the gas and liquid phases were generated by solving the differential equations describing the rate of change of tritium in the electrolyte, on the recombining electrode and in the gas phase. The simulated data were generated both with and without superimposed 1% Gaussian noise. Figure 5 shows the simulated data with superimposed 1% Gaussian noise for an a priori given cell current profile and low continuous production of tritium beginning on day 40. Analysis of the data set by computer–assisted fitting shows strong coupling between the adjustable parameters. The results are given in Table 3 and imply that, even for this simple case, the interpretation is ambiguous. Clearly, when the noise–free data are fitted for only the first 40 days (Table 3, column 1) the resulting values for the parameters are in excellent agreement with the values used to generate the data set. When the same procedure is applied to the noise–added case it shows a substantial degradation of the accuracy of the determined parameters (Table 3, column 2). When the data are expanded to include the last 10 days (Table 3, columns 3 and 4), i.e. when $q > 0$, the resulting fits decrease significantly in accuracy. Indeed, the plot shown in Fig. 5(b), for the residuals versus the day, is a clear indication of a failed fit attempt. The residuals are not Gaussian deviations but are clearly systematic. These deviations persist in the noise–added case (Fig. 5(c)), but are masked to a great extent by the noise.

One of the more interesting points regarding the 50 day computer analyses (Table 3, columns 3 and 4) is the evaluation of faradaic efficiencies greater than 100%. This results in the calculation of an artificially large replenishment volume. Consequently, additional amounts of tritium are added to the system and, in effect, the faradaic efficiency becomes a production term. Indeed, when this amount of "excess" tritium is calculated, it is actually larger (on an atoms per second basis) than the fitting parameter of q. This shows that in order to evaluate any value for the production (consumption) of tritium, great care must be taken with regard to the determination of all other parameters.

The computer program used to analyze the data was modified to include a parameter d which is the time at which tritium generation occurs. The results of this computer analysis are summarized in Table 3, column 5. Although the faradaic efficiency is greater than 100%, the computer analysis yielded a generation rate of 7837 atoms s^{-1} beginning on day 41.97. This compares remarkably well with the values used to generate the data set. A more sophisticated treatment is required to analyze examples of multiple bursts of tritium production; we have not yet investigated this situation.

4.2. Expected Versus Observed Behavior

The distribution of tritium between the "electrolytic" gas phase and the electrolyte arises from competition involving the various surface and bulk processes. In the absence of current (at equilibrium), this distribution is dictated by the equality of chemical and electrochemical potentials. With the current flowing, however, the separation factor is the dominant governing parameter in the distribution of tritium between the gas and liquid phases. Theoretical aspects of the separation factor have been thoroughly discussed by, among others, Bockris and Srinivasan [8] and Conway and Salomon [9], and those pertaining to the Pd/D system have been considered by Dandapani and Fleischmann [10].

When either eqn. (7) or eqn. (9) is employed, constancy of isotopic separation is assumed. It has been shown that, if tritium concentration data are available for both phases as a function of time, a curve–fitting technique provides a means of determining the value of the separation factor s. Application of this technique to several experimental runs has consistently yielded a separation factor of 1.8, which compares reasonably well with $s = 2$ reported in the literature [2,3]. Once the separation factor is known, the distribution of tritium between the gas and liquid phases can be calculated for any given cell current profile. If an excess of tritium is detected, its source, with either a constant or a

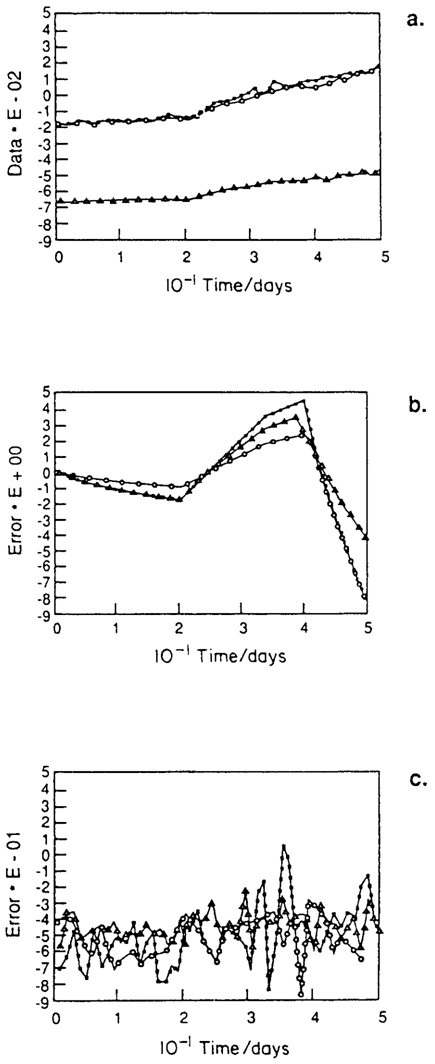

Figure 5. Summary of curve–fitting results for simulated data (see Table 3 for input parameters): (a) plots of data points and computer-generated curves as a function of time (this data set includes Gaussian noise); (b) plots of residuals (no Gaussian noise); (c) plots of residuals with 1% Gaussian noise on data. ■, liquid sample prior to addition of electrolyte to restore volume; ○, liquid sample after adding electrolyte; △, gas phase data.

Table 3. Computer analysis of simulated data.

	First 40 days, no noise	First 40 days with noise	All 50 days, no noise	All 50 days with noise	All 50 days [a] with noise
S	1.79959	1.80108	1.7989	1.79882	1.79429
ϵ_f	100.379	100.690	106.762	106.076	105.814
q/ (atoms s^{-1})	6.26512	1601.78	−1057.97	676.810	7837.44
Goodness of fit	1.00000	0.985501	0.993660	0.985784	0.988925
Commencement of ^3H generation	—	—	—	—	41.9715

Input data: $I = -50$ mA for 480 h, $I = -300$ mA for 720 h; $q = 10^4$ atoms s^{-1} for 240 h, commencing at 1680 h; $s = 1.8$, $\epsilon_r = 1.00$; $S^* = 1.00$, $\epsilon_f = 1.00$, $+q = 10^4$ atoms s^{-1}.

[a] In this computer analysis, the subroutine was modified to include a fifth parameter d, the time at which tritium production occurs.

time–dependent generation rate, can be located within either the interphase or the bulk electrode. Regardless of the location, magnitude and time dependence of the source, the fluxes leading to the distribution of tritium between the gaseous and liquid phases must originate at the adsorption plane. After the reduction of D_2O/DTO, three distinct transport paths are possible: (i) adsorbed T atoms can exchange only with D atoms of the D_2O molecules of the liquid phase; (ii) T atoms may enter the gas phase directly; (iii) adsorbed species may diffuse in the electrode interior. Path (iii) would strongly influence the distribution by controlling the concentration of adsorbed tritium and must therefore be considered whenever total mass balance is attempted. In practice, neither the constancy of tritium generation nor a single transport path can be assumed, thus making a detailed interpretation more speculative, as illustrated in Figs. 6 and 7 where Pd electrodes with two different surface, morphologies were employed. Figure 6 illustrates the distribution of tritium when the electrolysis was carried out on a dense metallic thin–film Pd electrode, while Fig. 7 summarizes the results obtained with a mossy dendritic electrode produced during the Pd/D code–position process [11].

Examination of the data presented in Fig. 6 shows that the tritium content in the electrolyte phase follows the calculated values within the limits of experimental error. Initially, the tritium content in the gas phase is much greater than that calculated for the isotopic separation factor. Such an increase in tritium content in the gas phase could be interpreted as evidence of tritium production. If this were the case, then the generated tritium would have to be transferred directly into the gas phase. In terms of the fluxes, this would mean that the surface processes leading to nucleation and growth of gas bubbles are faster than those responsible for tritium exchange with the incoming D2 O molecules (path (ii)). Another explanation could be offered, namely that the constancy of the *s* factor was not preserved within the time interval examined. Also, a time–dependent preferred absorption process into the uncharged electrode may account for the observed data. The existence of several possible explanations shows clearly that it is not possible, at this time, to come to a definitive conclusion regarding any possible tritium production/consumption.

We have applied the analysis to the tritium data reported by Bockris et al. [12] (Fig. 7). This distribution implies that the *s* factor is dependent on cell current and time, yielding a normal distribution, with $s = 2$ during the codeposition period (i.e. the first 80 h). Shortly after the cell current is tripled, a drastic change in the tritium distribution occurs and an excess of tritium appears in both phases. In terms of the model (eqns. (7) and (9)) tritium production has occurred with preferred transfer to the gas phase ($s = 1.2$). This situation remains unchanged until shortly before the next sampling (Fig. 7, point B). At this point, the tritium distribution yields an apparent *s* factor of 2.7. Assuming the constancy of the *s* factor, the model suggests burst–like production with preferred transfer to the electrolyte. The lower than expected tritium content in the gas phase would indicate that the burst occurred just before sampling (point B) since the reported tritium content is an average over the collection period. This high activity diminished with time and returned to normal with $s = 2.0$ (Fig. 7, point C).

The isotopic separation factor is a complex function representing the dynamics of the electrode–electrolyte interphase involving the various equilibria and transport and exchange processes [13]. Some variations in the *s* factor are thus expected. Whether or not a change from $s = 2.7$ to $s = 1.2$ is realistic and corresponds to the change in the dynamics for the same charging conditions remains an open question. Therefore it would appear that additional information (e.g. total mass balance) is highly desirable if definitive statements are to be made.

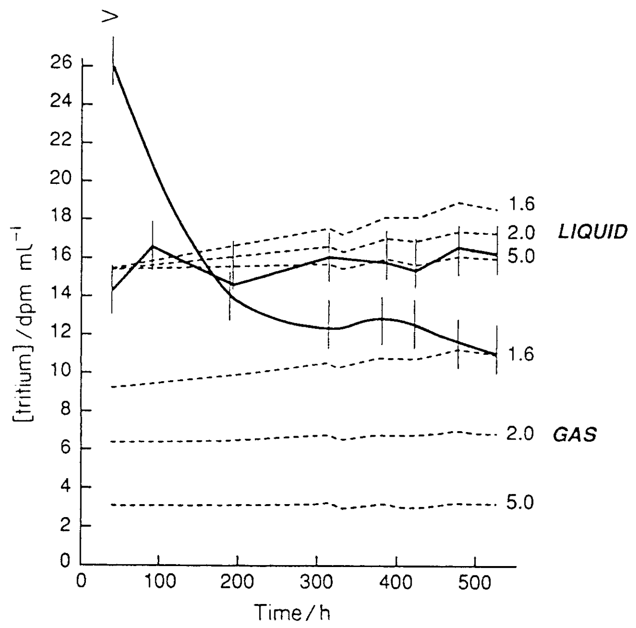

Figure 6. Tritium distribution as a function of time (electrode, thin film with a smooth surface prepared by electrodeposition; mode of operation, constant-current electrolysis in open cells): ———: computed distribution using the isotopic separation factors indicated; _______ measured tritium content in the electrolyte and gas phase.

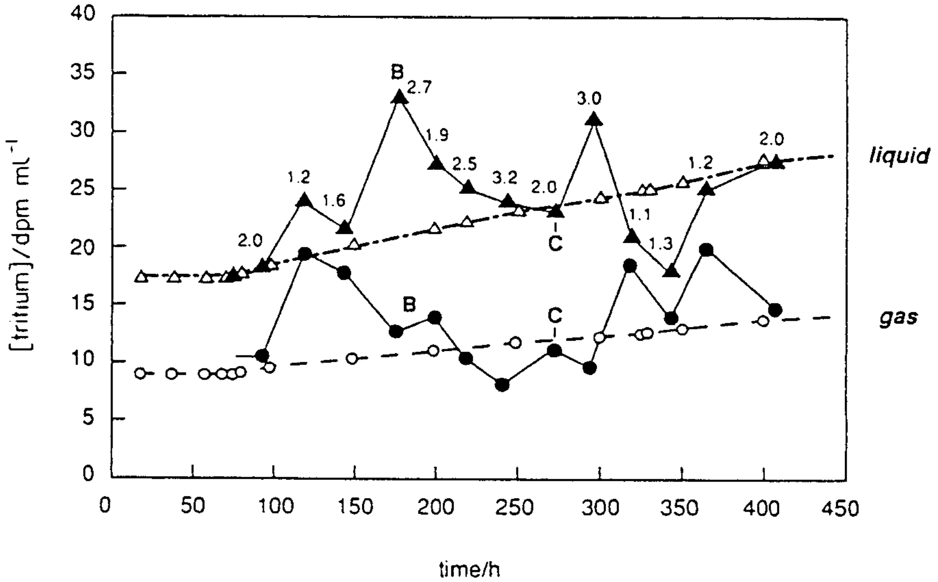

Figure 7. Tritium distribution as a function of time (electrode, prepared by codeposition from $PdCl_2$ solution; mode of operation, open cell with cell current profile indicated): ——— calculated distribution using *s* = 2.0; _____ experimentally measured tritium content (data from ref. 12). Experimental *s* values are indicated.

5. CONCLUDING REMARKS

An analysis of commonly employed experimental procedures and theoretical concepts has led to the following conclusions.

(i) Irrespective of the production term, the isotopic separation factor can be reliably determined by computer–aided analysis if tritium concentration data in both the gas and electrolyte phases are available.

(ii) Apparent changes in the isotopic separation factor, as a function of cell current and time, identify the dominant process(es).

(iii) The design of the "electrolytic" gas recombining vessel must assure that samples are representative of the total D_2O and DTO contents, i.e. the area of the catalytic surface must be sufficiently large to yield 100% efficiency.

(iv) The greatest source of error is the determination of tritium content, particularly at low concentrations. The error can be substantially reduced by increasing the counting time.

(v) When operating open cells with multiple samplings, care must be taken to assure good control of the electrolyte volume. Additional sampling is advisable to establish initial conditions for the next time interval accurately.

As a final closing remark, we should like to point out that one of the difficulties in providing irrevocable evidence of nuclear activities in open electrochemical cells via tritium analysis arises from, and is aggrevated by, intermittent and/or low generation rates. Such random events tend to prevent reproducibility despite a strict control of experimental conditions, and low generation rates could easily be too small to be reliably differentiated from zero. Therefore the most reliable method of determining tritium generation is through the use of closed cells, i.e. by taking the difference in tritium contents in all cell elements before and after completion of an experiment.

ACKNOWLEDGMENTS

The authors would like to thank Dr. C.J. Gabriel for computer analysis of the simulated data and Dr. D.R. Rolison for her comments during the preparation of this manuscript.

REFERENCES

1. M. Fleischmann, S. Pons and M. Hawkins, J. Electroanal. Chem.. 261(1989) 301.
2. E. Storms, Fusion Technol., 20(1991)433.
3. C.–C. Chien, D. Hodko, Z. Minevski and J. O'M. Bockris. J. Electroanal. Chem.. 338 (1992)189.
4. 4F.G. Will, K. Cedzynska, M.C. Yang, J.R. Peterson, H.E. Berge— son, S.C. Barrowes, W.J. West and D.E. Linton, Proc. 2nd Conf. on Cold Fusion, Como, 29 June—July 4 1991, Italian Physical Society, Bologna, 1991, p. 373.
5. S. Szpak, C.J. Gabriel, J.J. Smith and R.J. Nowak, J. Electroanal. Chem., 309 (1991) 273.
6. G.H. Un, R.C. Kainthla, N.J.C. Packham, O. Velev and J.O'M. Bockris, Int. J. Hydrogen Energy, 15 (1990) 537.
7. R.E. Adzic, D. Gervasio, I. Bae, B. Cahan and E. Yeager, Proc. 1st Annu. Conf. on Cold Fusion, Salt Lake City, UT, 28—31 March 1991, National Cold Fusion Institute.

8. J. O'M. Bockris and S. Srinivasan, J. Electrochem. Soc., III (1964) 844, 853, 858.

9. B.E. Conway and M. Salomon, Ber. Bunsenges. Phys. Chem.. 68 (1964) 331.

10. B. Dandapani and M. Fleischmann. J. Electroanal. Chem., 39 (1972) 323.

11. S. Szpak, P.A. Mosier—Boss and J.J. Smith, J. Electroanal. Chem., 302 (1991) 255.

12. J.O'M. Bockris, *C.C.* Chien, D. Hodko and Z. Minevski, Frontiers of Cold Fusion, Proc. 3rd Int. Conf. on Cold Fusion. October 1992, Nagoya, Universal Academy Press, Tokyo, 1993.

13. G. Sandrock, S. Suda and L. Schlapbach, Topics in Applied Physics, Vol. 2, Hydrogen in Intermetallic Compounds, Springer Verlag, 1992, Ch. 5.